Using τ_c to Estimate Magnitude for Earthquake Early Warning and Effects of Near-field Terms

Masumi Yamada

Pioneering Research Unit for Next Generation, Kyoto University, Uji, Gokasho, 611-0011, Japan

Jim Mori

Disaster Prevention Research Institute, Kyoto University, Uji, Gokasho, 611-0011, Japan

Abstract. This paper analyzes strong-motion records of 24 large earthquakes to investigate the relationship between τ_c (the period parameter of the first motion) and moment magnitude. The records of some of the large-magnitude events very close to the source include large near-field terms. Therefore, if we include the data with large near-field terms, we may overestimate the final size of the magnitude. We indentified records with large near-field terms, and did not include these data in processing the records to compute τ_c for each event. Our analysis shows that the value of τ_c is between the earthquake corner period and the period determined by the record duration τ_0. If the magnitude is less than 6, τ_c closely approximates the corner period, whereas τ_c for larger earthquakes depends on the rupture process and location of asperity. τ_c for large earthquakes provides a lower bound on the event magnitude, and approaches the corner period if a longer record is used.

We also propose a method to classify the records with and without large near-field terms. If the peak displacement amplitude for the first 3 seconds ($Pd3$) exceeds 1 cm and τ_c exceeds 2 s, the record is more likely to include large near-field terms.

For the purpose of quick onsite warnings, stations observing large near-field terms provide valuable information. Large near-field terms can be observed only if the magnitude is large and the epicentral distance is small. Therefore, if the displacement exceeds a threshold (e.g. $Pd = 0.5$ cm), the ground motion at the site would likely become very large. This criterion will help to issue warnings to the blind zone, which is the region where there is insufficient time to issue a warning before the strong shaking arrives.

1. Introduction

In October 2007, the Japan Meteorological Agency (JMA) launched a publicly available earthquake early warning system. It is one of the most extensively implemented systems in the world since it provides early warning to the public via TV and radio for the whole country.

Since the public release, JMA has issued warnings several times. The first one was for the Miyakojima-oki earthquake (M_j 5.2), which occurred near the islands 1000 km southeast of Honshu on May 12, 2008. The warning was issued 17 s after the origin time, but it overestimated the magnitude since the epicenter was actually closer to the closest station than the estimated location (with 50 km error). The station density was very sparse in those islands, so the quick and accurate determination of the epicenter was difficult.

The second event for which a warning was issued was the Ibaraki-oki earthquake (M_j 6.9), May 8, 2008. This is a subduction-zone earthquake, located 100 km east offshore of the Ibaraki prefecture, which should be optimal to issue an early warning. The determination of the epicenter was accurate within a 20 km error at 27 s after the origin time, but the magnitude was underestimated by 0.9. The estimated maximum seismic intensity was under the threshold to issue a warning until 80 s after the origin time had elapsed when the strong motions arrived across most of the severely shaken area.

0148-0227/17/$9.00

A current problem of the early warning system is its reliability in quick magnitude determination. The magnitude estimation of JMA is based on a magnitude-displacement relationship. Therefore, the initial magnitude estimate is usually an underestimate at the beginning, and grows as the fault rupture propagates. As long as the amplitude of the ground motion is used for magnitude estimation, the problem of initial underestimation is inevitable.

In order to improve the magnitude underestimation, this paper analyzes the τ_c method, which is another algorithm to determine the earthquake size. One of the merits of the τ_c method is that it uses the frequency content of the ground motion to estimate the size of the magnitude. The frequency component is usually more sensitive to the magnitude than ground motion amplitude in the initial few seconds of the P-wave, but the linear relationship with the magnitude for large earthquakes is still debated [Zoll et al., 2006, @; Rydelek et al., 2007, @; Wu and Kanamori, 2008b, @]. Olson and Allen, 2005 [@] proposed that the final magnitude of an earthquake is partially controlled by the initiation process within the first few seconds of the rupture, so the predominant frequency of the initial process scales with the final magnitude. Wu and Kanamori, 2005a [@] also shows that the τ_c scales with magnitude even for $M_w > 7$, without any obvious sign of saturation. On the other hand, recently, Rydelek et al., 2007 [@] processed a high-quality Japanese seismic network (Hi-net) dataset and showed that no trend between predominant frequency and magnitude is evident if $M_w > 6$. Also, Yamada and Ide, 2008 [@] came to similar conclusions considering models of earthquakes with complex ruptures.

In this paper we analyze strong-motion records of 24 large earthquakes. We investigate the effects of the near-field term

and the record duration used to compute τ_c, and provide a relationship between τ_c and magnitude that takes into account the possible presence of large near-field terms.

2. Strong-Motion Data

We used strong-motion datasets from 24 earthquakes with magnitudes greater than 6.0 and focal depths less than 100 km. The list of events is shown in Table 1. All inland events include at least one record within 50 km epicentral distance, and all events in subduction zones include at least one record within 150 km epicentral distance. Moment magnitudes from the Harvard CMT catalog are used.

The strong-motion dataset for the 1994 Northridge, 1999 Chichi, 1999 Izmit, 2002 Denali, and 2004 Parkfield events are the same as the dataset used by Yamada et al., 2007 [@]. The strong-motion dataset for the 1999 Hector Mine earthquake is provided by the U.S. Geological Survey seismic network and the Southern California Earthquake Center (SCEC) Data Center. The records of the aftershocks of the Chichi earthquake were provided by the Taiwan Central Weather Bureau Seismic Network. Strong-motion records of the 2008 Wenchuan earthquake were recorded by the China Earthquake Administration network. The records are available at the website of the China Earthquake Data Center (http://data.earthquake.cn). The Japan Agency for Marine-Earth Science and Technology (JAMSTEC) recorded the strong motions of the 2003 Tokachi-oki earthquake with seafloor accelerometers located above the shallow portion of the seismogenic zone. We used seismograms from three stations (KSL1, KSL2 and KSL3) for the mainshock, and one station (KSL1) for the aftershock in the offshore Kushiro-Tokachi network system (http://www.jamstec.go.jp/scdc/top_e.html). Data from the seafloor accelerometers may include both direct waves from the seismic source and reflections from the water or free surface, so we use the records of less than 3 s from the P-arrival.

The rest of the events which occurred in Japan were recorded by K-net and KiK-net operated by the National Research Institute for Earth Science and Disaster Prevention in Japan and the JMA strong motion network. The K-net and KiK-net data are available at their websites (http://www.k-net.bosai.go.jp/ and http://www.kik.bosai.go.jp/). JMA records are also available online. (http://www.seisvol.kishou.go.jp/eq/kyoshin/jishin/index.html) Since we are interested in near-source earthquakes, the records with epicentral distances greater than 150 km are not used.

3. Method

We processed the accelerograms obtained from 24 earthquakes according to the following procedure. The offset of the accelerograms is corrected by subtracting the mean of the pre-event portion of data. The records are integrated once in the time domain and high-pass filtered using a second-order one-way Butterworth filter with a corner frequency of 0.075 Hz. Note that this one-way Butterworth filter is recursive, so we can carry out this filtering in real time. The filtered velocity records are integrated once more in the time domain to obtain the displacement records.

The period parameter, τ_c, for a given duration of the beginning of the record is computed by the following equation [Kanamori, 2005, @; Wu and Kanamori, 2005a, @]:

$$\tau_c = 2\pi \sqrt{\frac{\int_0^{\tau_0} u^2(t)dt}{\int_0^{\tau_0} \dot{u}^2(t)dt}}, \quad (1)$$

where $u(t)$ is the vertical displacement high-pass filtered at 0.075 Hz, and τ_0 is the duration from the P-wave onset for each record (generally $\tau_0 = 3$ seconds). In this paper, various values of τ_0 are tested to check the effect of τ_0.

τ_c of each record is computed from the vertical acceleration component. For each event, the median of the closest 10 stations is selected to determine the value of τ_c. The value of τ_c depends on the site condition, radiation pattern, and other effects at each station. The effects of these factors on the determination of τ_c are not clear, and will be analyzed in more detail in future work. Here, we use the median of the 10 stations to remove this variance. Note that the 2002 Denali earthquake and 2008 Wenchuan earthquake have only a few near-source records. Therefore, τ_c of the Denali earthquake is the median of the closest 6 stations and τ_c of the Wenchuan earthquake is the value from only one station. Also, the Wenchuan record saturates in 5 s after the P-wave arrival, so values of τ_c for τ_0 equal to 10 and 20 s are not available.

4. Results and discussion

4.1. τ_c with τ_0 3 seconds

Figure 1 shows the relationship of the τ_c calculated with τ_0 equal to 3 s, as a function of moment magnitude for all 24 events. The median values of τ_c for the closest 10 stations are shown on the plot. This figure uses the same method as the results shown in Figure 2 of Wu and Kanamori, 2008b [@], but data which include large near-field terms have been removed.

In the Figure 2 of Wu and Kanamori, 2008b [@], τ_c seems to be strongly dependent on the magnitude, but the magnitude dependence of τ_c seems to be weaker in this figure. In our figure, there are some events with small τ_c and relatively large M_w (e.g. 1999 Hector Mine, 2000 Western Tottori, 2001 Geiyo, and 2002 Denali). The order of the Butterworth filter slightly changes the frequency content and may affect the relationship [Shieh et al., 2008, @], so we used the same filter as Wu and Kanamori, 2008b [@].

The dashed line shows the theoretical relations between the corner period and moment magnitude [Brune, 1970, @]. Assuming a circular fault of radius r, the corner period t_c (which is $1/f_c$, where f_c is the corner frequency) is given by Madariaga, 1976 [@];

$$t_c = \frac{r}{0.21 V_s} \quad (2)$$

Since the r scales with moment M_0 and stress drop $\Delta\sigma$ by $r = (\frac{7M_0}{16\Delta\sigma})^{1/3}$, the corner period is;

$$t_c = \frac{1}{0.21 V_s} \left(\frac{7M_0}{16\Delta\sigma}\right)^{1/3}. \quad (3)$$

Here, we assume $V_s = 4$ km/s and $\Delta\sigma = 10$ MPa. Since $M_0 = 10^{3/2(M_w+10.73)}$, $log_{10}t_c$ scales with $1/2M_w$. The dashed line in Figure 1 has the same slope with the corner period relation (Equation 3) and the intercept is determined to fit the data estimates of τ_c using τ_0 20 s, which should be an adequately long time window to accurately measure the actual corner period for all but the very largest events.

In our observations, the values of τ_c are in the shaded triangle area in Figure 1 and do not seem to follow a linear relationship. This can be explained as follows. The ruptures of small to moderate earthquakes ($M_w < 6.0$) are mostly contained within 3 s, so the estimation of τ_c gives values equivalent to the corner period and the data generally follow a relation close to the slope of the dashed line [e.g. Olson and Allen, 2005, @]. If the magnitude is greater

than about 6.0, the whole rupture is not contained in the first 3 s while the estimate of τ_c depends only on the beginning portion of the earthquake The earthquake may initiate with either large or small moment accumulation, depending on the locations of the areas of large slip. Earthquakes with small initial ruptures have smaller values of τ_c, such as for the 2002 Denali earthquake. If areas of large slip are close to the epicenter, τ_c becomes closer to the corner period (see Figure 2). Therefore, if τ_c is large, it indicates a large event, but a small τ_c may represent a lower limit value and then we will not know exactly the eventual size of the earthquake.

4.2. Effect of the value of τ_0

The purpose of the τ_c measurements is to quickly estimate the size of the earthquake, so there is trade-off between the speed of the estimate and using a longer time window, τ_0, for more reliable information. In order to characterize the effect of the value of τ_0, we determine τ_c using various values of the time window τ_0. The determination of τ_c using τ_0 equal to 10 s is shown in Figure 3. The rupture process of most earthquakes with magnitude less than 7 terminates within 10 s, so the value of τ_c approaches the corner period. τ_c of earthquakes with magnitude greater than 7 may also be close to the corner period, but depend on the rupture process. This relationship is shown by the shaded region in Figure 3. For earthquakes with magnitude less than 7, there is a general linear relation between magnitude and the log of τ_c. For earthquakes with magnitudes greater than 7, the value of τ_c can have any value greater than 2 s (this number corresponds to the lower bound of τ_c for earthquakes with magnitude greater than 7). For example, the 2003 Tokachi-oki earthquake is very large (M_w 8.3), and the rupture duration is much longer than 10 s. Therefore, the value of τ_c even using τ_0 equal to 10 s is still small compared to the total size of the magnitude. Although for this event, the S-wave has arrived at some of the near-source stations by 10 s after the origin time, so this estimate of τ_c is also contaminated by the effect of the S-wave.

Figure 4 shows the values of τ_c with τ_0 equal to 20 s. τ_c of most of the events with magnitude less than 7.5 approaches the corner period. Similar to Figure 3, the shaded area shows the region of expected values. Also, for comparison, the values of τ_c with τ_0 equal to 1 s are shown in Figure 5. There is a clear saturation of magnitude, and the range of τ_c spans only 1 to 3 s. The correlation between τ_c and magnitude is very weak in this figure. There is a limitation of the τ_c values for characterizing the initiation of the waveform and the exact physical meaning of τ_c is difficult to interpret [Simons et al., 2006, @; Wolfe, C., 2006, @]. However, we use this parameter as a simple estimate of the initial pulse duration.

From these observations, τ_c using τ_0 equal to 3 s represents the size of the magnitude if the event is smaller than magnitude 6. For larger earthquakes, τ_c would be less than the corner period and greater than the lower bound defined by τ_0. Using τ_c equal to 3 s seems to provide a reasonable threshold to identify large earthquakes that can cause shaking damage. In practice, a realtime system will likely have an initial estimate at 3 s, and frequent updates at intervals of one to several seconds.

4.3. Effect of the near-field term

The strong motions of large earthquakes very close to the fault include long-period components and static displacements. These are the near-field terms, that begin to arrive at the same time as the P-wave. Figure 6(a) shows typical records with large near-field term components, and 6(b) shows records with little near-field contributions. It is clear that the near-field term is long period (often monotonically increasing) between P- and S-wave arrivals.

The effect of the near-field term has not been considered for the magnitude estimation so far [Allen and Kanamori, 2003, @; Wu and Kanamori, 2008a, @]. However, recent studies show the near-field term may contaminate magnitude estimation significantly [Wu and Kanamori, 2008b, @]. McGuire et al., 2008 [@] pointed out the importance of the near-field term on earthquake early warning applications using a wavelet analysis, although their study did not provide a comprehensive evaluation. To examine the influence of the near-field term, we distinguished the data that contain large near-field terms by identifying the records with clear ramps between the P- and S-waves in the displacement records.

Figure 7 shows the relationship between τ_c and magnitude for the records with and without large near-field terms. Values of τ_c for the records with large near-field terms are larger than those without near-field terms, so they tend to overestimate the magnitude.

Some of the 1999 Chichi earthquake records include large near-field terms, so if these records are included, the value of τ_c becomes longer than if only the direct P waves were used. This overestimated τ_c places the Chichi earthquake on the linear trend in Wu and Kanamori, 2005a [@]. The slip at the beginning of the Chichi earthquake is relatively small [Ji et al., 2003, @], which should have resulted in a value of τ_c which is relatively small compared to its final magnitude. τ_c of the 2004 Niigata-ken Chuetsu earthquake would also be overestimated if we had included the records with large near-field term.

From Figure 7, if τ_c exceeds 3 s, it is either due to a large near-field term or a very large earthquake. However, it is difficult to distinguish between these two cases. Figure 8 shows the range of epicentral distance and magnitude for which the near-field term is dominant in the records. The amplitude of the near-field term depends on the magnitude, radiation pattern, initial rupture, and epicentral distance. This figure shows the near-field term tends to be large if the magnitude is large, and the epicentral distance is small.

In order to classify the records with and without large near-field terms, the combination of τ_c and peak displacement of the first 3 s ($Pd3$) is effective. Figure 9 shows the relationship between τ_c and $Pd3$. If $Pd3$ exceeds 1 cm and τ_c exceeds 2 s, the record is more likely to include a large near-field term. Therefore, to accurately estimate the earthquake size from τ_c, the records with large near-field terms should not be used. At the same time, for the purpose of quick on-site warnings, stations observing large near-field terms provide valuable information. Note that we do not have enough records with large near-field terms for earthquakes with magnitude greater than 7.6 (see Figure 8). Therefore, we are not sure if this classification criterion can be applied for the very large earthquakes. Wavelet analysis is one of the alternative procedures to characterize large near-field terms [McGuire et al., 2008, @].

Wu and Kanamori, 2005b [@] proposed an on-site warning criterion for a threshold P-wave displacement of $Pd = 0.5$ cm. If the displacement exceeds this value, the ground motion at the site would likely become very large. Figure 10 shows the peak ground velocity (PGV) of the vertical component and the time after the P-wave arrival for the vertical displacement to exceed $Pd = 0.5$ cm. Most of the records with large near-field terms exceed 0.5 cm within 2 s, and some exceed the threshold in less than one second. There are a few misclassified records that exceed this threshold but produce small PGV less than 10cm/s, such as 2004 Kushiro earthquakes, which occurred in the offshore subduction zone with no data within 50km from the hypocenter. However, the overall success rate for issuing warnings is satisfactory. This criterion will help to issue warnings to the blind zone that is close to the source and for which it is difficult to

obtain an event location and magnitude before the S wave arrives.

The advantage of this threshold warning using near-field terms is that it can be quick and does not require the information from other stations (i.e. a single station warning). The current earthquake early warning system provided by JMA is a network-based approach, and multiple records are processed simultaneously to determine the magnitude and location. On the other hand, this on-site approach uses available data at a given site to predict the local ground motion. This method is suitable for the region close to the epicenter, since it can provide a warning to the area faster than the network-based approach. If we incorporate this algorithm into the real-time strong motion stations, the on-site approach can issue a very quick warning, and the network-based approach can later issue more location and magnitude based information. For practical applications, we may have to solve some technical problems, but we hope that this approach will provide quicker warning for the region close to the source.

5. Conclusions

This paper analyzes strong motion records of 24 large earthquakes to investigate the relationship between τ_c (the period parameter of the first motion) and moment magnitude. We investigate the effects of the near-field term and the record duration used to compute τ_c, and provide a relationship between τ_c and magnitude for data that do not contain large near-field terms.

We analyzed the records which do not have large near-field waveforms, and computed τ_c for each event. The value of τ_c for the first 3 s of the P-wave gives a lower bound of the magnitude. If the magnitude is less than 6, τ_c is close to the corner period, whereas τ_c for larger earthquakes depends on the rupture process and locations of areas of large slip. In practice, if the value of τ_c is large, the earthquake must be large with large slip near the epicenter. If the value of τ_c is small, the event may be a small earthquake, or may be a large earthquake that grows later. τ_c for large earthquakes approaches the corner period, if a sufficiently long record duration is used.

Fortunately, the near-field term for large earthquakes becomes very clear in the 3 s after the origin time, so the classification of the record with and without large near-field terms is possible. One of the ways to do this is to measure both the peak displacement and τ_c. We propose a method where records with Pd3 exceeding 1 cm and τ_c exceeding 2 s, are more likely to include a large near-field term.

For the purpose of quick on-site warnings, stations observing large near-field terms provide valuable information. Large near-field terms can be observed only if the magnitude is large and the epicentral distance is small. Therefore, if the displacement exceeds a threshold (e.g. $Pd = 0.5$ cm), the ground motion at the site would likely become very large. This criterion will help to issue warnings to the blind zone that is close to the source.

Acknowledgments. We are deeply appreciative of comments provided by the associate editor, reviewers, and Dr. Hiroo Kanamori whose detailed comments greatly improved this manuscript. We thank all the institutions providing strong motion data, especially the COSMOS data center, SCEC data center, NIED and JMA. This research was supported by the Program for Improvement of Research Environment for Young Researchers from Special Coordination Funds for Promoting Science and Technology (SCF) commissioned by the Ministry of Education, Culture, Sports, Science and Technology (MEXT) of Japan.

References

Allen, R. and H. Kanamori (2003), The Potential for Earthquake Early Warning in Southern California. *Science, 300*(5620), 786–789.

Brune, J. (1970), Tectonic Stress and the Spectra of Seismic Shear Waves from Earthquakes. *J. Geophys. Res., 75*(26), 4997–5009.

Ji, C., D. Helmberger, D. Wald, and K. Ma (2003), Slip History and Dynamic Implications of the 1999 Chi-Chi, Taiwan, Earthquake. *J. Geophys. Res., 108*(B9), 2412, doi:10.1029/2002JB001764.

Kanamori, H. (2005), Real-time Seismology and Earthquake Damage Mitigation. *Annual Review of Earth and Planetary Sciences, 33*(1), 195–214.

Madariaga, R. (1976), Dynamics of an Expanding Circular Fault. *Bull. Seismol. Soc. Am., 66*(3), 639–666.

McGuire, J., F. Simons, and J. Collins (2008), Analysis of Seafloor Seismograms of the 2003 Tokachi-oki Earthquake Sequence for Earthquake Early Warning. *Geophys. Res. Lett., 35*, L14310, doi:10.1029/2008GL033986.

Olson, E. and R. Allen (2005), The Deterministic Nature of Earthquake Rupture. *Nature, 438*(7065), 212–215.

Rydelek, P., C. Wu, and S. Horiuchi (2007), Comment on "Earthquake Magnitude Estimation from Peak Amplitudes of Very Early Seismic Signals on Strong Motion Records" by Aldo Zollo, Maria Lancieri, and Stefan Nielsen. *Geophys. Res. Lett., 34*, L20302, doi:10.1029/2007GL029387.

Shieh, J., Y. Wu, and R. Allen (2008), A Comparison of τ_c and τ_p^{max} for Magnitude Estimation in Earthquake Early Warning. *Geophys. Res. Lett., 35*, L20301, doi:10.1029/2008GL035611.

Simons, F., B. Dando, and R. Allen (2006) Automatic detection and rapid determination of earthquake magnitude by wavelet multiscale analysis of the primary arrival. *Earth and Planetary Science Letters, 250*(1-2), 214–223.

Wolfe, C. (2006) On the Properties of Predominant-Period Estimators for Earthquake Early Warning. *Bull. Seismol. Soc. Am., 96*(5), 1961–1965.

Wu, Y. and H. Kanamori (2005a), Experiment on an Onsite Early Warning Method for the Taiwan Early Warning System. *Bull. Seismol. Soc. Am., 95*(1), 347–353.

Wu, Y. and H. Kanamori (2005b), Rapid Assessment of Damage Potential of Earthquakes in Taiwan from the Beginning of P waves. *Bull. Seismol. Soc. Am., 95*(3), 1181–1185.

Wu, Y. and H. Kanamori (2008a), Development of an Earthquake Early Warning System Using Real-time Strong Motion Signals. *Sensors, 8*, 1–9.

Wu, Y. and H. Kanamori (2008b), Exploring the Feasibility of On-site Earthquake Early Warning Using Close-in Records of the 2007 Noto Hanto Earthquake. *Earth, Planets and Space, 60*(2), 155–160.

Yamada, M., T. Heaton, and J. Beck (2007), Real-time Estimation of Fault Rupture Extent Using Near-source versus Far-source Classification. *Bull. Seismol. Soc. Am., 97*(6), 1890–1910.

Yamada, T. and S. Ide (2008), Limitation of the Predominant-period Estimator for Earthquake Early Warning and the Initial Rupture of Earthquakes. *Bull. Seismol. Soc. Am., 98*(6), 2739–2745.

Zollo, A., M. Lancieri, and S. Nielsen (2006), Earthquake Magnitude Estimation from Peak Amplitudes of Very Early Seismic Signals on Strong Motion. *Geophys. Res. Lett., 33*, L23312, doi:10.1029/2006GL027795.

M. Yamada, Kyoto University, Uji, Gokasho, 611-0011, Japan (masumi@eqh.dpri.kyoto-u.ac.jp)

Earthquake	Date	Latitude	Longitude	Depth(km)	M_w
Northridge	1994/01/17	34.21	-118.54	18.0	6.6
Kobe	1995/01/17	34.59	135.04	17.9	6.9
Izmit	1999/08/17	40.75	29.86	17.0	7.6
Chichi-1	1999/09/20	23.81	120.85	8.2	7.6
Chichi-2(aftershock)	1999/09/20	23.81	120.86	8.2	6.4
Chichi-3(aftershock)	1999/09/20	23.61	120.81	1.1	6.4
Chichi-4(aftershock)	1999/09/22	23.83	121.05	15.6	6.4
Chichi-5(aftershock)	1999/09/25	23.85	121.00	12.1	6.5
Hector Mine	1999/10/16	34.59	-116.27	0.0	7.1
Western Tottori	2000/10/06	35.27	133.35	9.0	6.7
Geiyo	2001/03/24	34.13	132.69	46.5	6.8
Denali	2002/11/03	63.52	-147.44	4.9	7.8
Northern Miyagi	2003/05/26	38.82	141.65	72.0	7.0
Tokachi-oki-1	2003/09/26	41.78	144.08	27.0	8.3
Tokachi-oki-2(aftershock)	2003/09/26	41.71	143.69	21.4	7.3
Kii-1	2004/09/05	33.03	136.80	37.6	7.2
Kii-2	2004/09/05	33.14	137.14	43.5	7.4
Parkfield	2004/09/28	35.81	-120.38	5.5	6.0
Mid Niigata-1	2004/10/23	37.29	138.87	13.1	6.6
Mid Niigata-2(aftershock)	2004/10/23	37.31	138.93	14.2	6.3
Kushiro	2004/11/29	42.95	145.28	48.2	7.0
West off Fukuoka	2005/03/20	33.74	130.18	9.2	6.6
Off Miyagi	2005/08/16	38.15	142.28	42.0	7.2
Noto Hanto	2007/03/25	37.22	136.69	10.7	6.7
Niigata-ken Chuetsu-oki	2007/07/16	37.56	138.61	16.8	6.6
Off Ibaraki	2008/05/08	36.17	141.72	88.3	6.8
Wenchuan	2008/05/12	30.99	103.36	19.0	7.9
Iwate-Miyagi Nairiku	2008/06/14	39.03	140.88	11.9	6.9

Table 1. List of the earthquakes used for the analysis. Moment magnitude (M_w) is cited from the Harvard Centroid Moment Tensor solution.

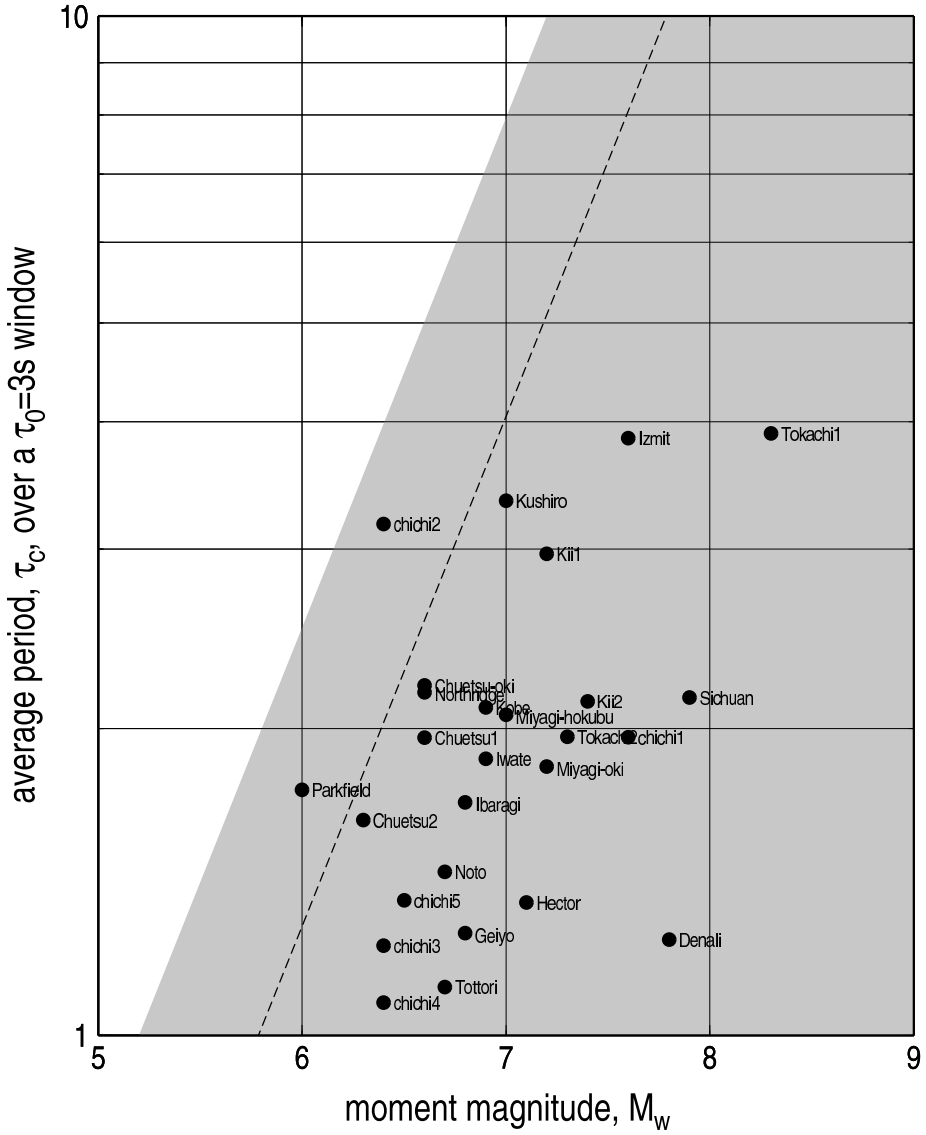

Figure 1. Relation between moment magnitude (M_w) and period parameter (τ_c) using τ_0 equal to 3 s. The shaded area shows the possible values of τ_c. The dashed line shows the theoretical relation between magnitude and corner period.

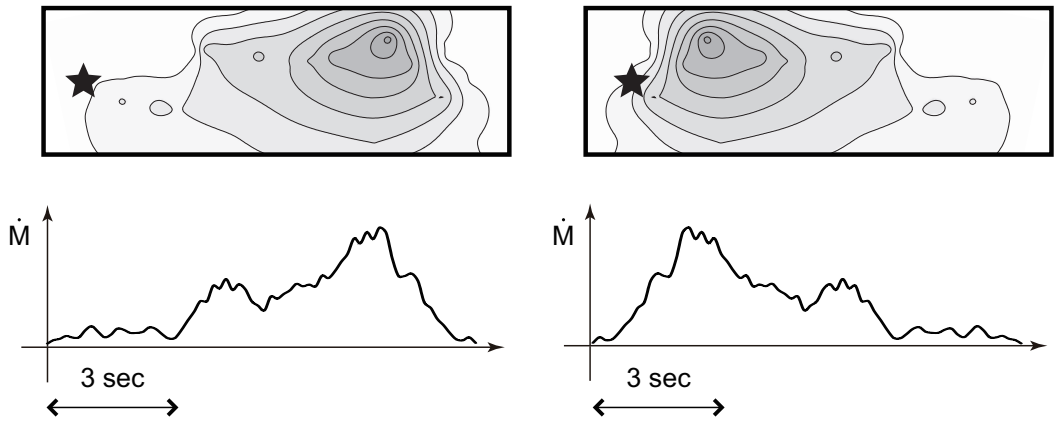

Figure 2. Schematic diagrams of the slip distribution and moment-rate function. Earthquakes with small initial ruptures (left figure) have smaller values of τ_c. If areas of large slip are close to the epicenter (right figure), τ_c becomes closer to the corner period. Stars in the slip distribution indicate the epicenter.

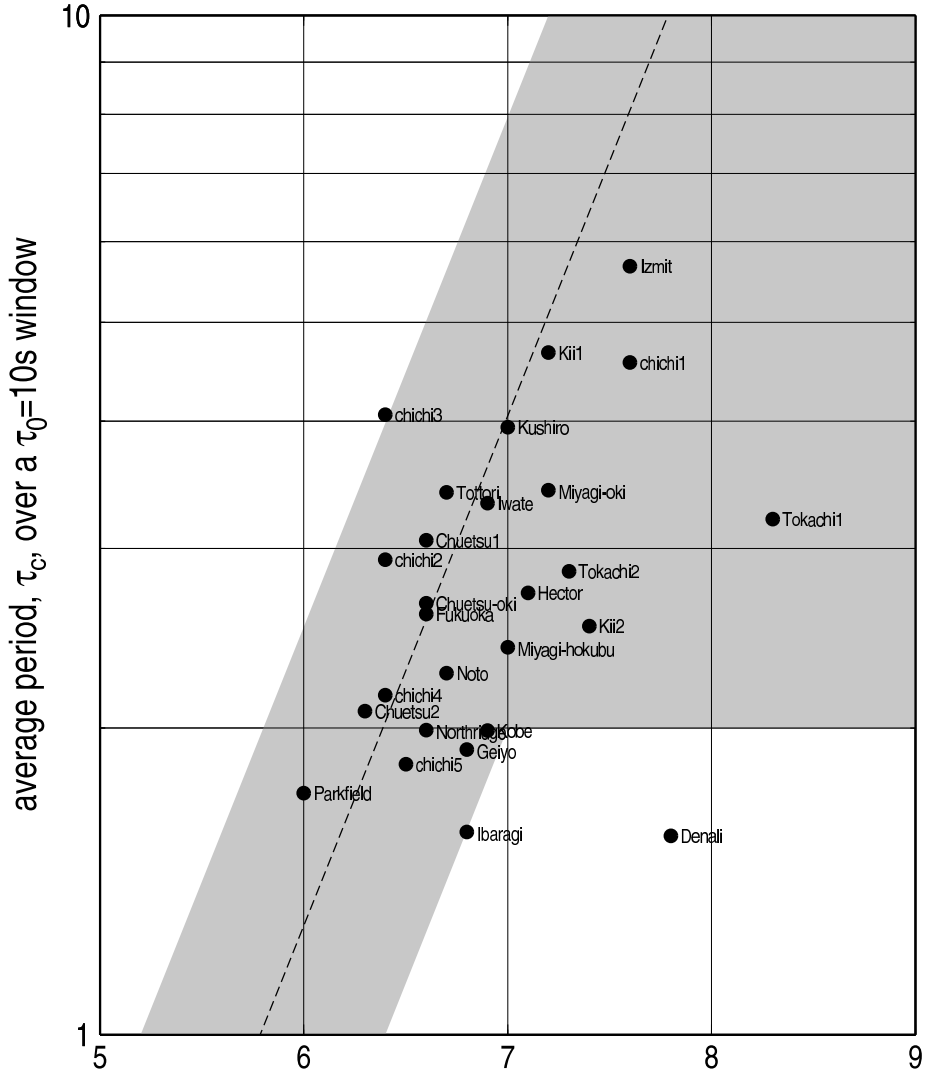

Figure 3. Relation between moment magnitude and τ_c using τ_0 equal to 10 s. The symbols are the same as in Figure 1.

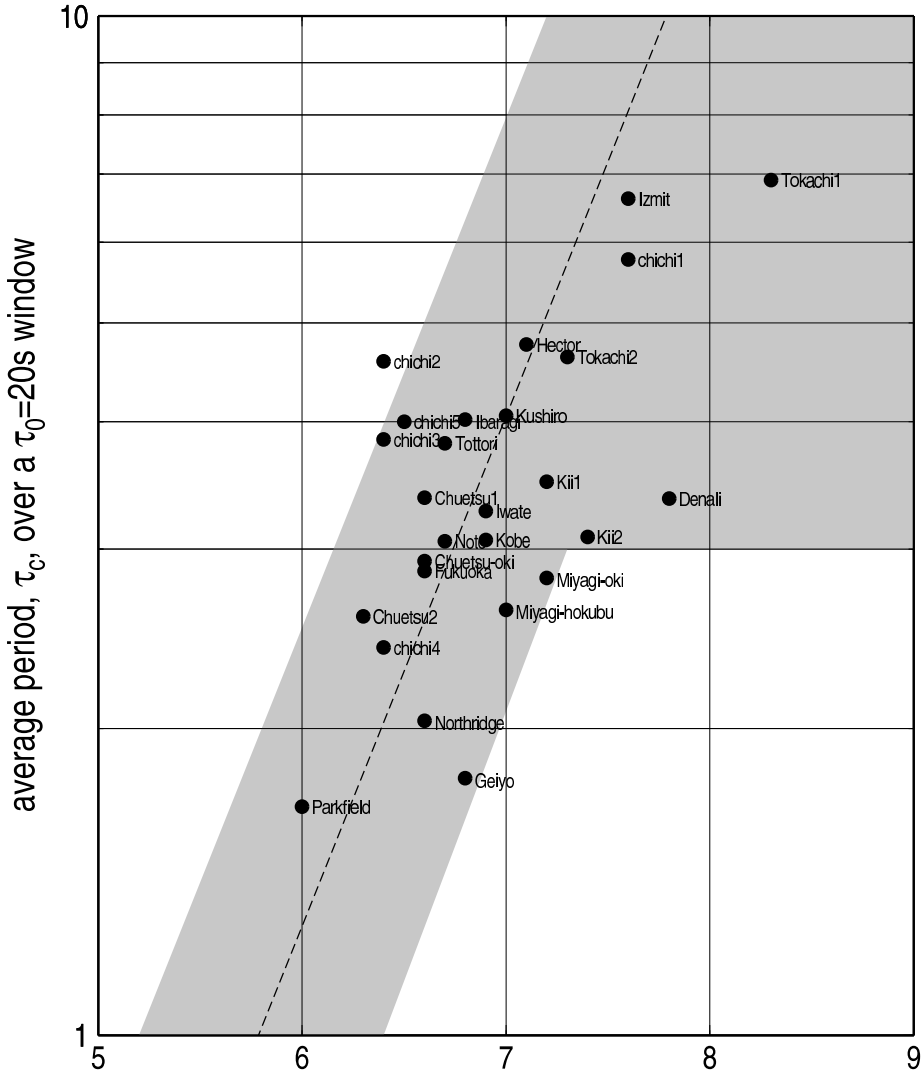

Figure 4. Relation between moment magnitude and τ_c using τ_0 equal to 20 s. The symbols are the same as in Figure 1.

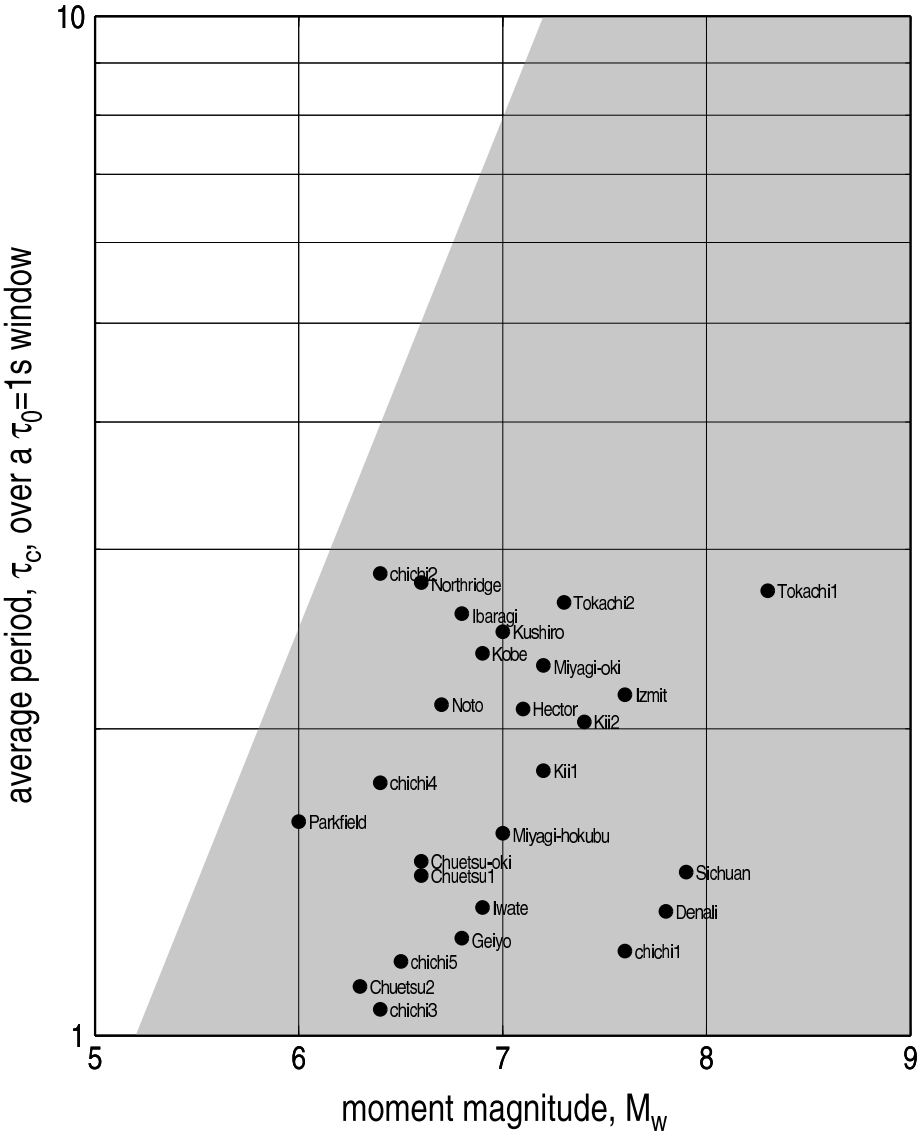

Figure 5. Relation between moment magnitude and τ_c using τ_0 equal to 1 s. The symbols are the same as in Figure 1.

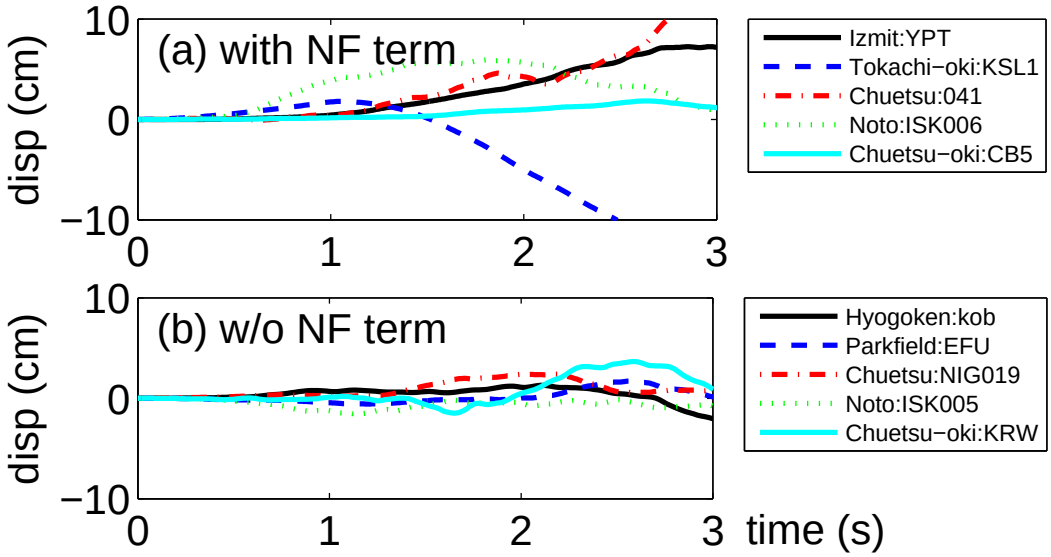

Figure 6. The first 3 s of the displacement records (a)with large near-field term and (b) without large near-field term. The zero of the X-axis is the initial P arrival.

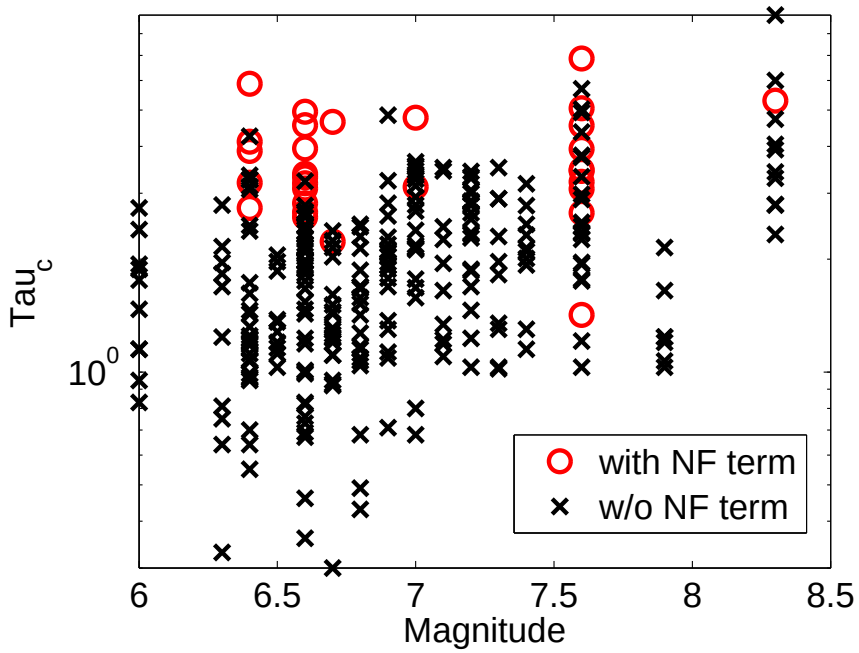

Figure 7. Magnitude and τ_c using τ_0 equal to 3 s for each record in this study. The circle and cross symbols indicate data with and without large near-field terms, respectively.

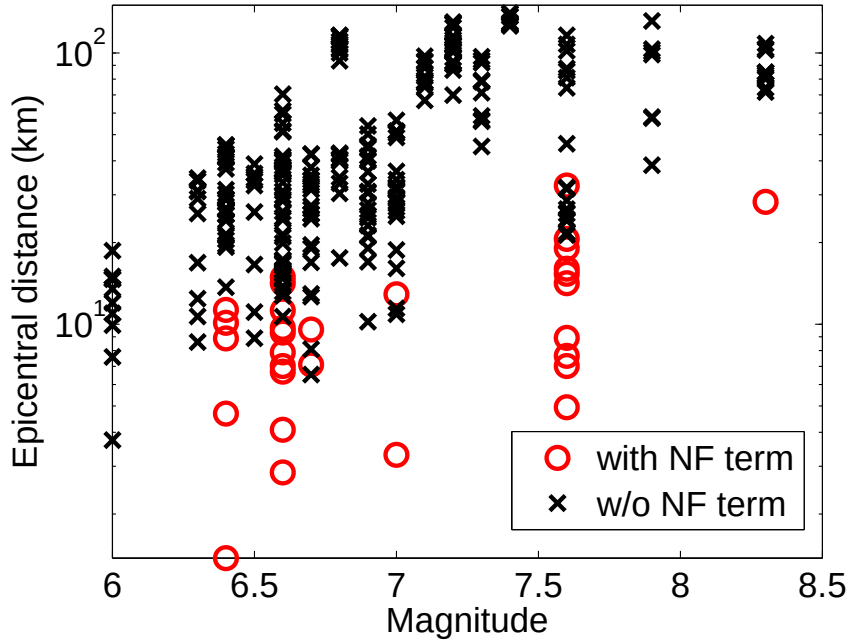

Figure 8. Magnitude and epicentral distance of stations that recorded data used in this study. The symbols are the same as in Figure 7.

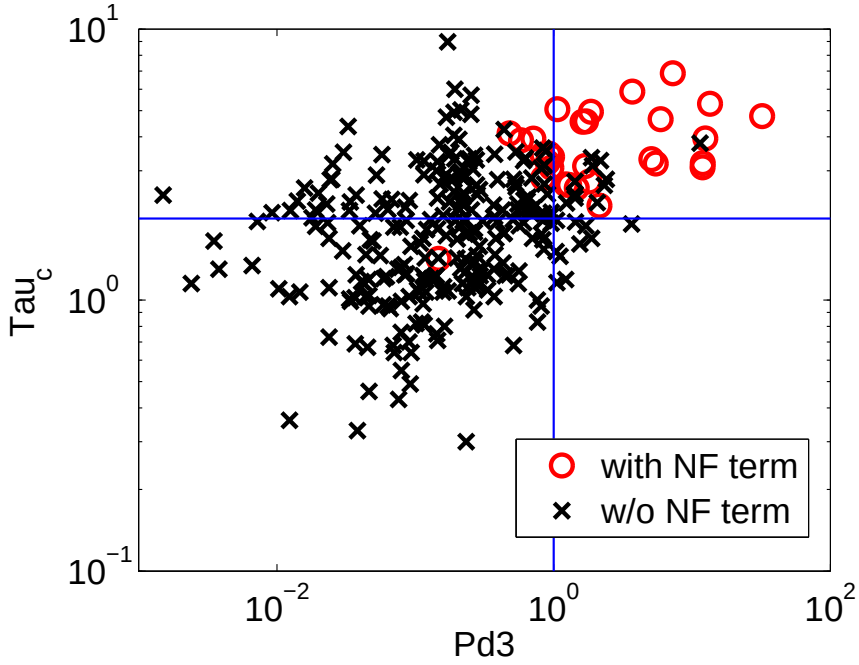

Figure 9. $Pd3$ and τ_c using τ_0 equal to 3 s for each record in this study. The symbols are the same as in Figure 7.

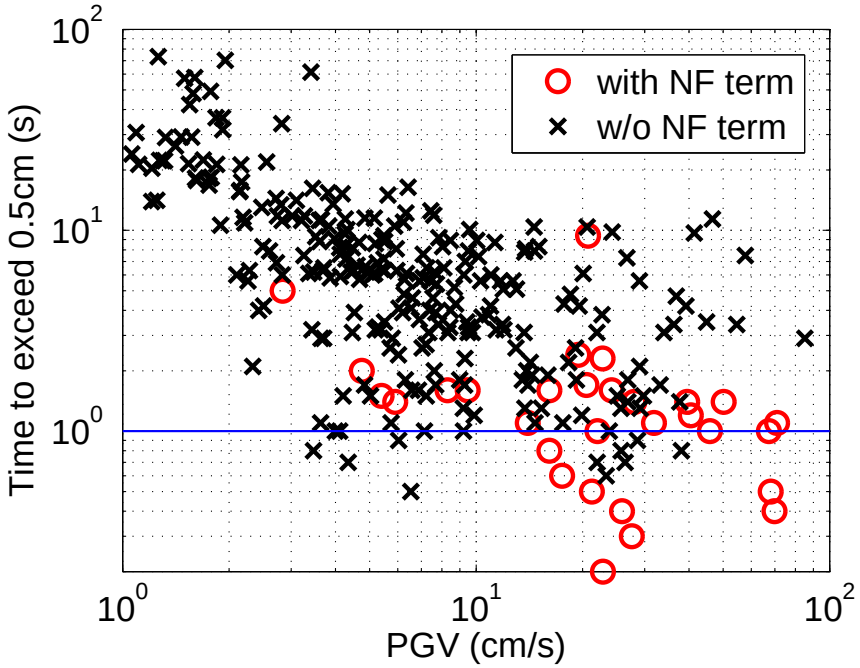

Figure 10. PGV and the time after the P arrival for the vertical displacement to exceed Pd = 0.5cm. The symbols are the same as in Figure 7.